ACADEMIC PRESS

Available online at www.sciencedirect.com
SCIENCE DIRECT®

Journal of Colloid and Interface Science 265 (2003) 106–114

JOURNAL OF Colloid and Interface Science

www.elsevier.com/locate/jcis

Structural and acidic characteristics of Cu–Ni-modified acid-leached mordenites

Mohamed Mokhtar Mohamed

Chemistry Department, Faculty of Science, Benha University, Benha, Egypt

Received 17 October 2002; accepted 14 January 2003

Abstract

Two series of dealuminated Na-mordenite zeolites (DML and DMH) were impregnated, in comparison with the parent nondealuminated NaMSP, in aqueous nitrate solutions of Cu and Ni to achieve varying loadings for both of the cations. These samples were characterized by N_2 adsorption, XRD, DSC of ammonia desorption, ammonia volumetric sorption, IR of ammonia adsorption, and FTIR-photoacoustic (FTIR-PAS) techniques. The FTIR-PAS spectrum of CuNi-loaded NaMSP shows a band at 935 cm^{-1} ascribed to $O_3Si–O–SiO_3$ linkages produced as a result of dealumination caused by the synergistic effect of Cu and Ni cations under the preparation conditions. As a confirmation, this band was intensified upon acid dealumination (DML) where, at the extent of dealumination (DMH), collapsing of the zeolite structure was obtained subsequent to cation modification. In addition, the dealumination effect was markedly enhanced upon increasing the load of Cu in proportion to Ni. A total erosion of OH group characteristics of Si–(OH)–Al at 3610 cm^{-1} was depicted when the Ni content exceed that of Cu where it did not show any change when the Cu content surpasses that of Ni. The amount of adsorbed ammonia measured volumetrically was enlarged after dealumination as well as after increasing the contents of the modificating cations. The IR study of ammonia adsorption revealed a band at 1428 cm^{-1}, in either nondealuminated or dealuminated-modified samples, assigned to stronger Bronsted acid sites than those at 1455 cm^{-1}. The band at 1428 cm^{-1} was markedly enhanced in the latter samples than in the former. This was due in part to the replacement of the protons by cations, producing sufficiently mobile protons. In conformity, ΔH values obtained for DSC effects via ammonia desorption were enhanced after dealumination. Other correlations with XRD and surface texturing on one hand and the structural variations following cations incorporation on the other hand are evaluated and discussed.

Keywords: Cu–Ni encapsulation; Na-mordenite; Dealumination; XRD; N_2 adsorption; Volumetric adsorption of ammonia; DSC; FTIR-PAS

1. Introduction

The current interest in the family of silica-based mesoporous materials, designated as M41S [1], is in large part due to their large surfaces, abundant pore volumes, and hydrophobic surface properties. The main drawback of these materials is their inactive chemical composition. Therefore, modification of the surface is essential to endow the M41S materials with desirable properties such as catalytic or environmental. Some attempts have been made to modify specific candidates of this family such as MCM-41 or FSM-16 with B, Al, Ga, and Fe [2–5]. It has been reported generally that the structural regularity of M41S materials was markedly decreased with increasing metal ion contents beside the formation of cristobalite (SiO_2) crystals; i.e., some of silica are not involved in the structure during synthesis [6]. Further studies have revealed a sharp decrease in hydrothermal stability along with considerable loss in BET surface area [7].

On the other hand, the microporous alumino-silicate mordenite zeolite specifically after dealumination has had increasing attention due to the following: 1, mordenite can be dealuminated to a high degree without losing its crystallinity; 2, dealumination is known to modify the activity as well as the microporous volume and the external surface of the zeolite; 3, an increase in the number of strongly acidic sites. Accordingly, the dealuminated mordenite was chosen as a substrate for incorporating transition metal ions such as Cu and Ni due to its structural, i.e., active chemical composition, and acidic properties, which indeed are superior to the corresponding analogue in mesoporous materials [8]. Because of the debate and speculation concerning the presence of nonstructural Al and whether or not it possesses

E-mail address: mohmok2000@yahoo.com.

0021-9797/$ – see front matter
doi:10.1016/S0021-9797(03)00075-4

acidic properties [9], dealumination via acid leaching only was carried out in this work. After acid dealumination, a unidirectional channel system accessible through quasi-circular 12-membered ring windows can be created in addition to the formation of secondary mesopore network within the channels of the zeolite [10]. The latter network favors the transport of reactants and products in the crystals and thus reduces the toxicity by coke. The introduction of mesopores in mordenite could provide the accessibility of a large amount of molecular reactant into the active site [11].

Previous reports have shown that Cu–Ni oxides supported on silica show a remarkable selectivity in the isomerization of *n*-hexane and the hydrogenation of ethylene and butadiene [12–14]. Thus, this study is designed to gain information concerning the effect of the residual tetrahedral aluminum on the encapsulation of Cu–Ni.

The aim of the current study is twofold: 1, to provide details of the structural changes that take place after dealumination and incorporation of Cu–Ni atoms; and 2, to provide information about acidity variation and its strength following dealumination and metal ion incorporation. This information is a necessary prelude to further study of the catalytic properties of dealuminated modified zeolites that will be described in a subsequent publication.

2. Experimental

2.1. Catalyst preparation

The starting material, sodium small-port mordenite (NaMSP) of unit cell $Na_{8.9}[(AlO_2)_{8.9}(SiO_2)_{40.1}]$ supplied by La Societe Chimique De La Grand Pavoisse, was acid-leached under two different acid concentrations (2.5 and 5.0 mol dm^{-3} HCl). The dealumination was performed at a reflux temperature of 373 K for 3 h. The samples were then washed in flowing distilled water to get rid of chloride ions, dried overnight at 373 K, and crushed to less than 75-μm particle size. The dealuminated samples that were designated as DML and DMH, respectively, were calcined at 723 K in air (0.5 K min^{-1}) over a period of 48 h prior to cation incorporation in order to avoid any dealumination sequences from the self-steaming process. The total aluminum contents of dealuminated NaMSP, analyzed by classical chemical analysis, are listed in Table 1. The zeolite-loaded Cu and Ni were prepared by impregnation of nondealuminated and dealuminated mordenites with aqueous solutions of copper and nickel nitrates at the desired wt% of each. These samples were dried at 393 K for 12 h and calcined at 773 K in air for 24 h at a rate of 0.5 K min^{-1}. The samples were, respectively, referred to as xCuyNi/NaMSP for nondealuminated, and xCuyNi/DML and xCuyNi/DMH for dealuminated ones. The suffixes x and y refer to the loading of Cu and Ni in weight percentages, respectively.

2.2. Characterization techniques

The IR spectra were recorded on a Nicolet 5-DXB FTIR spectrometer equipped with a METC-100 photoacoustic detector (PAS). The spectra were recorded with 4 cm^{-1} resolution and a mirror velocity of 0.16 cm s^{-1}, and 500 scans were averaged. After calcining the samples they were stored in a glove box purged with dry nitrogen enclosing the photoacoustic cell (PA), which is continuously flushed with ultradry helium, that was finally positioned in the IR equipment for collecting the spectra. The photoacoustic detector is able to study all types of solid materials, especially zeolites, without the need for difficult sample pretreatment. The time-consuming techniques for grinding and pressing self-supporting wafers are evaded. Spectral information over the full IR region can be obtained; even changes in the lattice vibrations can be investigated without making use of KBr disks. Scattering effects have no influence on the spectra so that various sizes of crystallites can be investigated without the problems of baseline changes [15].

The volumetric sorption of ammonia onto calcined samples was performed at 423 K till equilibrium is attained up to a final pressure of 1 Torr. However, a quantitative ammonia adsorption can be measured at every dose.

After completion of the volumetric measurements a careful outgassing (10^{-4} Torr) at 423 K for 0.5 h for all the samples was carried out and then the samples were placed in the dry nitrogen glove-box with the PA cell to collect the IR spectra.

X-ray diffraction spectra were obtained using Cu$K\alpha$ radiation on a Philips X-ray spectrometer. The data were

Table 1
Total Al contents, unit cell parameters, and N_2 adsorption data of various samples

Sample	Acid-leaching procedure	Al_t (mmol g^{-1})	S_{BET} (m^2 g^{-1})	V_m (ml g^{-1})	Cell constants (Å)			Volume (Å^3)	Crystallinity (%)
					a	*b*	*c*		
NaMSP	Parent	2.5	463	0.2263	18.16	20.51	7.50	2793.5	100
DML	NaMSP + 2.5 mol dm^{-3} HCl, 3 h, 373 K	2.2	496	0.2161	18.21	20.32	7.47	2764.1	91
DMH	NaMSP + 5.0 mol dm^{-3} HCl, 3 h, 373 K	1.8	523	0.2695	18.12	20.40	7.47	2761.3	82
6Ni1Cu/NaMSP	NaMSP + 6 wt% Ni +1 wt% Cu	2.3	483	0.2301	18.20	20.70	7.47	2828.2	91
6Ni1Cu/DML	DML + 6 wt% Cu +1 wt% Ni	2.0	470	0.2239	18.20	20.52	7.49	2797.2	89
6Cu1Ni/DML	DML + 6 wt% Cu +1 wt% Ni	1.8	431	0.2053	17.85	19.85	7.29	2588.8	76

The crystallinity was obtained from the sum of the intensities of the 111, 130, 241, 511, and 530 diffraction lines. The original NaMSP is taken as reference at 100% crystallinity. Volume is the unit cell volume $a * b * c$. Al_t is the number of total Al in mmol g^{-1}. V_m is the total pore volume.

recorded from $2\theta = 6$ up to 46 °C at 2 °C min^{-1} and at room temperature.

Differential scanning calorimetry (DSC) measurements were performed on a DSC-50 (Shimadzu). The problem in measuring thermodesorption from zeolite by DSC was solved by performing the desorption run with Al metal as a reference and maintaining the sample at the end temperature until a stable signal was reached [16]. The sample was cooled down without opening the cell and a 50 $m^3\,min^{-1}$ NH_3–N_2 flow was applied and the sample was scanned at 10 K min^{-1} up to 823 K.

3. Results and discussion

3.1. IR study of dealuminated mordenites

Figure 1 shows the IR spectra of different dealuminated Na-mordenite zeolites (DML and DMH) in comparison with the nondealuminated one (NaMSP). As it can be seen, the structural bands (450–900 cm^{-1}) showed some variations as a result of dealumination. For instance, the bands at 457 and 580 cm^{-1} that are characteristic of the zeolite framework showed almost no change in their positions but they displayed a decrease in intensities along with splitting at the extent of dealumination (DMH), e.g., the 580 cm^{-1} splited into 562 and 601 cm^{-1} bands. This splitting could be associated with varying the energy of the residual Al ions present in 5 rings as a result of dealumination. This is confirmed from the band broadening which is usually taken as a measure of heterogeneity. The band at 638 cm^{-1} showed a decrease in intensity accompanied by broadening and an upward shift in wavenumbers to 650 cm^{-1} to verify that it is due to Al–O in alternating SiO_4 and AlO_4 tetrahedra [17]. The symmetrical stretching vibration of T–O at 800 cm^{-1} showed an increase in intensity with almost no change in position where the 710(739) cm^{-1} band (inverted band) was almost vanished at the extent of dealumination. A small band at 880 cm^{-1} was depicted in the Na-MSP sample and appeared as a shoulder in the DML spectrum. This shoulder was not apparent in the DMH spectrum. Accordingly, this band could be associated with TO_4 tetrahedra in [O–(Al,Si)–O] or in Si–O–Si involved structures. These assignments are not supported by the present results because of the disappearance of the band with dealumination; besides, no increase in intensity or wavenumbers was detected as a result of the expected replacement of lost Al by Si. Thus, it is likely attributed to external symmetric stretching vibrations.

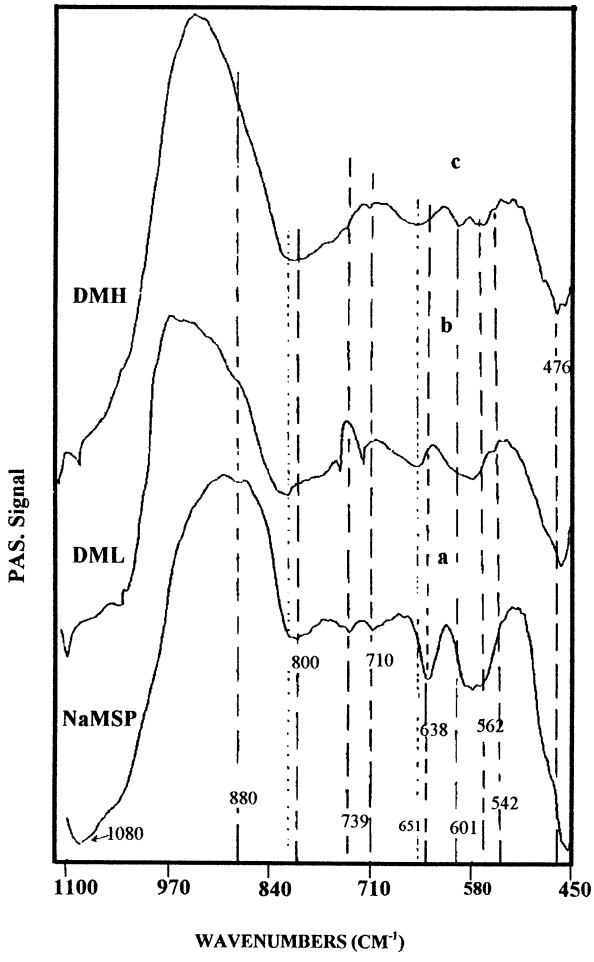

Fig. 1. PAS spectra of nondealuminated (NaMSP) and dealuminated (DML and DMH) mordenite zeolites.

3.2. IR study of Cu–Ni-encapsulated dealuminated mordenites

Figure 2 shows the IR spectra of nondealuminated (NaMSP) and dealuminated Na-mordenites (DML and DMH) loaded 1 wt% Cu–1 wt% Ni. The spectrum of CuNi/NaMSP showed marked spectral changes compared with that of NaMSP (Fig. 1) in the 450–1100 cm^{-1} region. A marked decrease in intensity along with splitting of the bands at 460, 560, and 640 cm^{-1} was depicted upon metal ion incorporation. This indicates the existence of Cu and Ni ions in stabilized sites inside mordenite channels apparently in positions near the 5-membered rings due to the distortion and change of symmetry of these rings (560 cm^{-1}). The 720 cm^{-1} is not affected by CuNi incorporation; however, the high-frequency symmetric band (810 cm^{-1}) becomes well resolved and distinct. On the other hand, the symmetrical T–O-stretching band seen at 880 cm^{-1} (Fig. 1) was depicted at 851 cm^{-1} upon cation incorporation as a result of lattice relaxation effects [18]. Of particular interest, a band at 935 cm^{-1} was observed in the CuNi/NaMSP spectrum. This band was not apparent in the NaMSP spectrum (Fig. 1). Accordingly, it is associated with the presence of the modifying cations.

The dealuminated samples encapsulating CuNi revealed the following features when compared with those of either NaMSP or CuNi/NaMSP samples. First, the splitting of the bands that appeared in the latter sample (Fig. 2) was completely removed upon dealumination, resulting in spectra similar to those obtained in Fig. 1 prior to cation incorpo-

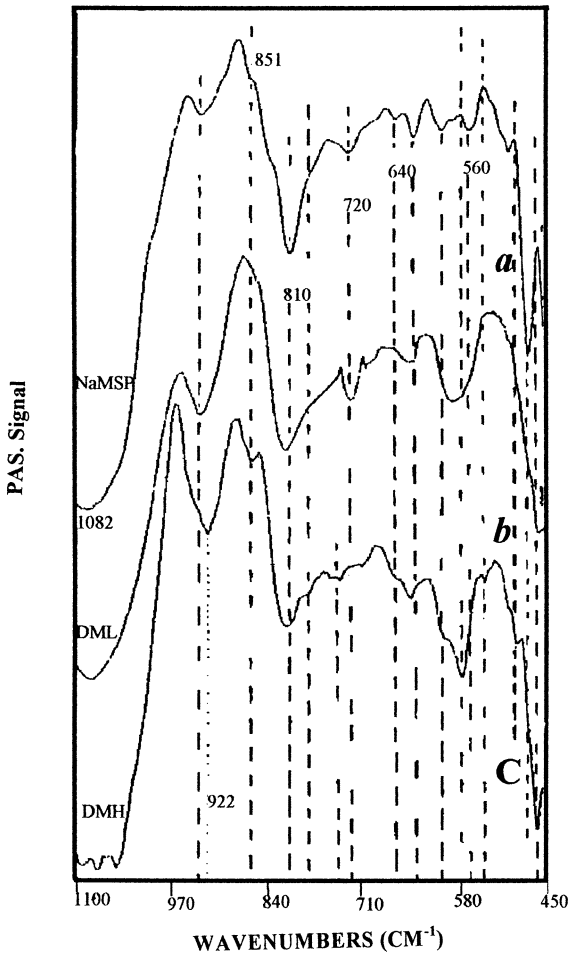

Fig. 2. PAS spectra of nondealuminated and dealuminated mordenite loaded 1 wt% Cu 1 wt% Ni.

ration especially in the region below 900 cm^{-1}. However, a decrease in intensity along with a shift to higher wavenumbers was depicted for 640 and 720 cm^{-1} bands in addition to the vanishment of the latter at the extent of dealumination. This confirms the higher sensitivity of these sites to dealumination and to cation exchange. The resemblance of dealuminated spectra before and after cation addition concludes the good incorporation of the cations in dealuminated samples, i.e., highly dispersed cations in the dealuminated one.

The band at 935 cm^{-1} seen in CuNi/NaMSP spectrum was intensified and showed a shift to lower wavenumbers with the extent of dealumination (DMH, 922 cm^{-1}). This band was produced upon CuNi addition (Fig. 2) either in nondealuminated or dealuminated samples. Thus, it is likely correlated with the presence of the modifying cations. However, it is improbable assigning this band to either CuO or NiO species that used to have bands in the 600–650 cm^{-1} region. This was confirmed by the absence of any lines appointed to oxide species in the XRD patterns (not shown). One can speculate that this band 935(922) cm^{-1} is due to the formation of monovalent copper or nickel ions produced as a result of autoreduction processes that could be facilitated by water as follows:

$$H_2O + M^{2+} + ZO^- \rightarrow [M(OH)^+] + ZOH,$$

$$2[M(OH)]^+ \rightarrow 2M^+ + H_2O + \tfrac{1}{2}O_2.$$

However, exposing the CuNi/NaMSP sample to CO at room temperature for 30 min did not show any band around 2145 cm^{-1}, characteristic of M^+(Cu or Ni)–CO (not shown). Thus, suggesting the presence of a band, as, for example, due to $Cu(OH)^+$ of a frequency at 900 cm^{-1} is not supported by the preceding experiment [19]. When mordenite is dealuminated by acid leaching, simultaneous extraction of vicinal Al atoms occurs, resulting in the formation of silanol defect sites (SiOH groups) at 935 cm^{-1} with no evidence of residual amorphous alumina [20]. However, the presence of the same defect sites in the nondealuminated zeolite sample (Fig. 2, CuNi/NaMSP spectrum) leads to the conclusion that assigning this band to νSi–OH is inconceivable. Accordingly, one can assign the 935(922) cm^{-1} band to $O_3Si–O–SiO_3$ bonds. This means that under such treatment conditions Cu and Ni ions manipulate the dealumination of NaMSP. Indeed, this has been evidenced in major work of pentasil zeolite containing copper during either hydrothermal treatment or during NO_x reduction [21]. However, so far no IR study has recorded such behavior. Thus, indeed the presence of Ni beside Cu could bring about the dealumination under the circumstances of the preparation conditions. As a confirmation for the previous assignment, a band at 955 cm^{-1} due to $O_3Si–O–SiO_3$ bonds was found in dealuminated mordenite [22]. The evident shift of the band from 935 to 922 cm^{-1} with dealumination is a result of the influence of water contained inside zeolites that indeed was substantiated after acid leaching.

Figure 3 shows the effect of increasing the Cu loading in proportion to Ni and their effects on the IR spectral consequences of nondealuminated and dealuminatd samples. It can be seen that increasing the Cu loading (6 wt%) over that of Ni (1 wt%) in the NaMSP sample especially in the region below 900 cm^{-1} causes no changes in position or in intensity, resulting in a spectrum similar to the cation-free NaMSP. This indicates the dispersion of CuNi inside the mordenite channels. The reason can be explained by inspecting the band at 930 cm^{-1} that has been intensified if compared with the one seen for 1 wt% Cu–1 wt% Ni/NaMSP (Fig. 2). This indicates the enhancement of the dealumination process in the former sample compared to the latter. This suggests that increasing the copper contents enhances progressively the dealumination that was responsible for exhibiting the dispersion for the cations (Fig. 3). On the contrary, increasing the load of Ni over that of Cu did not show any consequences of dealumination enhancement (not shown). This result emphasizes our assignment of attributing this band to $O_3Si–O–SiO_3$ linkages. In the 6 wt% Cu–1 wt% Ni/DML spectrum (Fig. 3), the total intensity for the range 450–640 cm^{-1} is not much affected; however, the band at 720 cm^{-1} was completely vanished. This indicates the involvement of the metal ions in the vicinity of the framework

Al [23]. Since, the 720 cm^{-1} band is associated with the framework Al in mordenite, its disappearance is a sign of the dealumination event. No significant changes are detected for the 930 cm^{-1} band, indicating probably the limit of dealumination. On the other hand, the 6Cu1Ni/DMH spectrum showed the collapsing of the zeolite structure. This can be due to the additional dealumination that caused by CuNi cations. This was responsible for an evolution of a band at 1035 cm^{-1} due to ν_{as}Si–O– that can be used as criteria for the partial detaching of SiO_2 from T–O [24]. As a further confirmation, a marked decrease in the unit cell volume of this sample, if compared with all samples, with increasing Cu contents was depicted reflecting the poor incorporation of Cu in the mordenite framework (Table 1).

The contribution of cationic unexchangeable Al^{VI} species to the vibration mode of the 930(922) cm^{-1} band resulted from dealumination caused by CuNi cations, considering that leaching is not capable of removing all Al nonframeworks originated from acid dealumination is of small preponderance. This is because of the downward shift of Al–O frequencies when the coordination number of Al is changed from 4 to 6 (670–760 cm^{-1}) [25]. Besides, aluminate spinels with either Cu or Ni or both, considering that the experimental conditions allow their formation, have frequencies in the 680–750 cm^{-1} region [25]. The synergy behavior of the bands at 850 and 930 cm^{-1} suggests that they are of similar species or at least highly related ones. Thus, the tendency of assigning this band to Al^{IV}–O species is invalid.

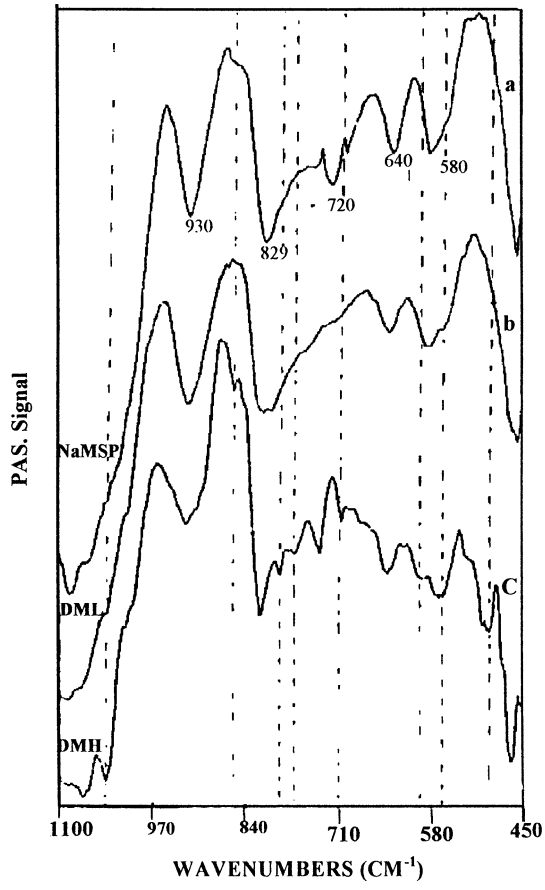

Fig. 3. PAS spectra of nondealuminated and dealuminated mordenite loaded 6 wt% Cu 1 wt% Ni.

3.3. Surface hydroxyl groups

Figure 4 shows the IR spectra in the hydroxyl-stretching region (3800–3100 cm^{-1}) for dealuminated mordenites (DML and DMH) before and after cation encapsulation.

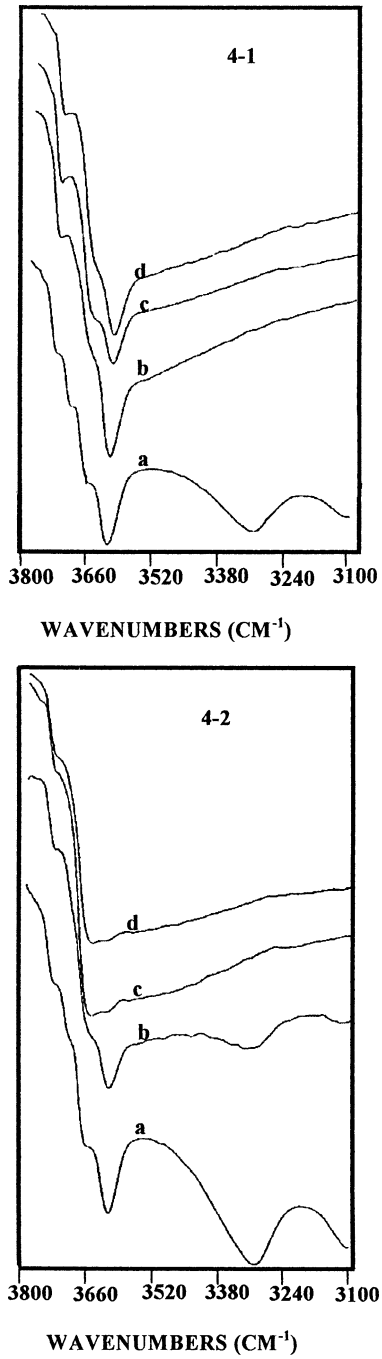

Fig. 4. Transmission spectra of OH-stretching frequencies of dealuminated mordenites (DML, 4-1, and DMH, 4-2) loaded CuNi: a, unloaded samples; b, 6 wt% Cu 1 wt% Ni; c, 1 wt% Cu 1 wt% Ni; d, 6 wt% Ni 1 wt% Cu.

The spectrum of the DML sample (Fig. 4-1) is characterized by bands at 3733 and 3690 and a sharp intense band at 3610 cm^{-1} due to internal-bridged Si–(OH)–Al groups [26]. This spectrum also exhibits a very broad band at 3310 cm^{-1} that was extended to 3240 cm^{-1}. By analogy with dealuminated Na-mordenite and Na-ZSM-5 zeolites [27,28], this band is assigned to vibrations of internal silanol located at defect sites (≡SiOH. . .HOSi≡) and interrupted by water molecules. In the CuNi-exchanged samples (see curves c and d) the band of the bridged Bronsted sites is markedly decreased in intensity while its persistence in curve b points to either the lower acidity of the site or to the insignificant effect of copper atoms. This insignificant effect of Cu atoms could be associated with their presence in small pores (6 or 8 rings) since the 3610 cm^{-1} band represents the bridging hydroxyl groups in the large pores of mordenite (12 rings) [29]. The terminal framework silanol band at 3733 cm^{-1} was intensified at the expense of vanishing the band at 3690 cm^{-1} that can be ascribed to residual Al–OH groups [30]. This confirms that the external Si–OH groups are practically unaffected by CuNi dosage where a correlation between divalent cations and the 3690 cm^{-1} band can be obtained together with the band at 3310 cm^{-1} that has disappeared completely upon cation exchange. This suggests the interaction of the bivalent cations with the OH groups of perturbed silanol replacing water molecules.

On the other hand, Fig. 4-2 of the DMH sample showed marked variations after cation incorporation when compared with that of Fig. 4-1. A total erosion of the 3610 cm^{-1} band (Fig. 4-2, curves c and d) indicates that the bivalent cations and specifically Ni ones have substituted nearly all protons on the internal bridged Si–(OH)–Al sites. This could also indicate the preference of Ni cations to be located in internal –Si–(ONi)–Al– bridged positions if compared with those of Cu. This can be ascertained by the prominent existence of the bands at 3310 and 3610 cm^{-1} in the 6Cu1Ni/DMH sample revealing that Cu^{2+} can not effectively eliminate such sites especially the acidic one (3610 cm^{-1}). This could be associated with the smaller diameter of Ni–H_2O complex than that of Cu one at the very beginning of the exchange and thus the preferential location of Ni^{2+} to such sites took place. The intensity of the interrupted Si–OH groups at 3310 cm^{-1} was much higher in the DMH spectrum than that in DML. This could be taken as an indication of the lower degree of ordering in the zeolite and of the evolution of mesoporsity showing a low degree of connectivity leading to a large number of internal ≡SiOH–(Q^3)– and also some =Si(OH)$_2$–(Q^2)– groups [31]. The weaker intensity of the 3690 cm^{-1} in the DMH than DML spectrum emphasizes our assignment for this band to the residual Al in the mordenite framework. Of particular interest, the Si–OH band at 3733 cm^{-1} is unaffected by cation exchange. This observation argues against finding the bands at 3733 and 3690 cm^{-1} as a merged profile as proposed by Sayed et al. [32]. From the preceding results, one may suggest that CuNi are present at the Al sites (3690 cm^{-1}) and the replacement of the Bronsted protons with Ni cations (3610 cm^{-1}) was maximum if compared with that of Cu.

3.4. IR study of adsorbed ammonia

Figure 5 shows the IR spectra in the region of N–H-bending vibrations below 1730 cm^{-1} of NH_3 adsorbed on nondealuminated (Fig. 5-1) and dealuminated (Figs. 5-2 and 5-3) mordenite encapsulated CuNi samples. Spectrum 5-1a depicts an IR band at 1632 as well as split band at 1407 and 1373 cm^{-1}. The band at 1632 cm^{-1} is characteristic of NH_3 bonded to Lewis acid sites together with the one

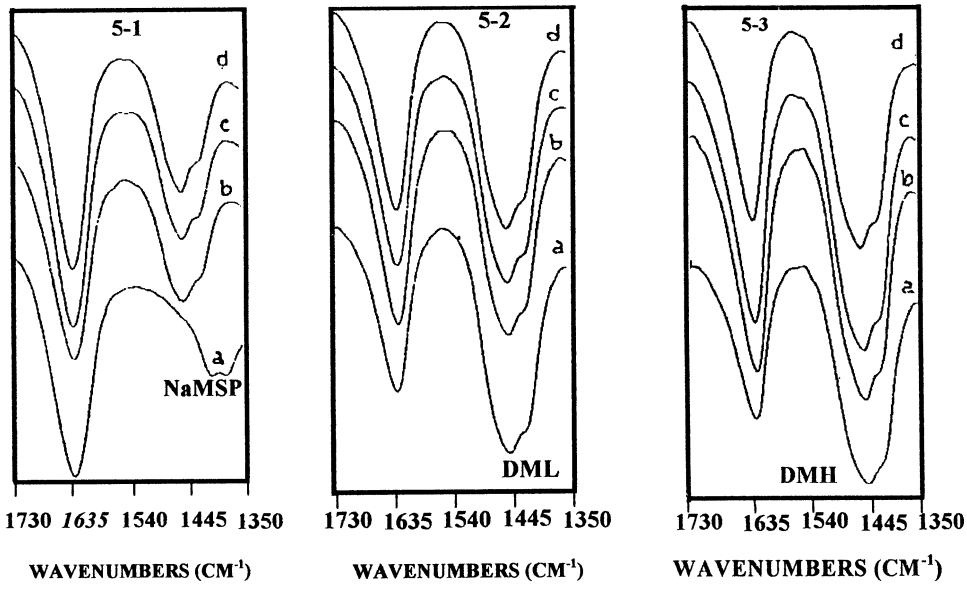

Fig. 5. IR spectra in the N–H-bending region of ammonia adsorbed on nondealuminated (NaMSP, 5-1) and dealuminated mordenite (DML, 5-2, and DMH, 5-3) zeolite loaded CuNi at 423 K: b, 6 wt% Ni 1 wt% Cu; c, 1 wt% Cu 1 wt% Ni; d, 6 wt% Cu 1 wt% Ni.

at 1373 cm^{-1} [33], whereas the band at 1407 cm^{-1} is due to ammonium cations arising from the protonation of ammonia on Bronsted acid sites [34]. The bands at 1407 and 1373 cm^{-1} showed a shift to higher wavenumbers (1455 and 1422 cm^{-1}) upon CuNi incorporation (spectra 5b–d). This establishes that the frequencies of symmetric deformation (in-plane bending) vibration ($\delta_s = 1373\ cm^{-1}$) are the most sensitive followed by the frequency of asymmetric deformation vibration ($\delta_{as} = 1407\ cm^{-1}$) to metal cations [35]. Increasing δ_s on transition from nondealuminated to CuNi-modified nondealuminated indicates an increase in the proportion of strong electron-accepting centers on the surface of the latter, i.e., formation of the coordination bond enhances the force constant and the frequency of the symmetric deformation vibrations. On the other hand, the trend underlying the shift of the δ_{as} NH^{4+} frequency into the high frequency from 1407 to 1455 cm^{-1} points to the weakening of Bronsted acid centers in the CuNi-modified nondealuminated mordenites. Interestingly, the 1632 cm^{-1} band showed only a shift to 1629 cm^{-1} with perceived changes in intensity. It can be seen that the amount of ammonia adsorbed at Lewis sites (1632 cm^{-1}) enhanced significantly when the copper ratio exceeds that of Ni despite the acknowledged information regarding Cu^{2+} that points to its lower power of electron-acceptor property. This could be due to the adsorption of ammonia on pairs of adjacent Cu^{2+} sites [36]. As a plausible explanation, site geometry may result in a different coordination of Cu ions that would create different adsorption sites with ammonia molecules [37].

The spectra of ammonia adsorbed on dealuminated modified samples (Figs. 5-2 and 5-3) showed bands comparable to those of nondealuminated modified ones (curves b–d) at 1629, 1452, and 1428 cm^{-1}. A nearly constant loss in intensity of the 1629 cm^{-1} is observed with dealumination (Figs. 5-2a and 5-3a), indicating a marked decrease in the amount of ammonia bound to such Lewis sites. The intensity of these sites increases upon modification (Figs. 5-2 and 5-3, b–d), exhibiting a small shift to lower wavenumbers (1626 cm^{-1}) approaching those of coordinated ammonia to either Cu^{2+} or Ni^{2+} ions [38].

On the other hand, the sites at 1452 and 1428 cm^{-1} in Figs. 5-2 and 5-3 act more strongly toward ammonia than those in Fig. 5-1. Thus, it is unlikely that the 1428 cm^{-1} band is assigned to Lewis acid sites due to the enhancement in its intensity following dealumination (Figs. 5-2a and 5-3a) in addition to its synchronizing behavior attached with the band at 1452 cm^{-1} ascribed to NH^{4+}. Therefore, the 1428 cm^{-1} band can be devoted to other Bronsted acid centers produced as a result of dealumination. This points to the strength of Bronsted acid centers in the latter (1428 cm^{-1}) if compared with that at 1452 cm^{-1}. Interestingly, the latter bands showed an enhancement upon modification, although of the established weak proton donation of employed cations. This could be due to the replacement of the protons by cations producing sufficiently mobile protons or due to M(Cu or Ni)O–H that can hardly be detected. Similarly, Cu-exchanged Na-ZSM-5 also produced Bronsted acidity [37].

3.5. Volumetric adsorption of ammonia

Figure 6 shows the isotherms of ammonia adsorption at 423 K on various samples. Generally, for each sample, the isotherm steeply increases at low pressure and runs almost parallel to each other yielding different amounts of irreversible adsorbed ammonia that can easily be estimated from the figure. With the extent of dealumination (curve c), the amount of ammonia adsorbed is enlarged up to a factor of 2.0 if compared with the nondealuminated sample (curve a). This is a consequence of the enlargement of void volume as a result of dealumination, as seen in Table 1. It seems also that the increases in S_{BET} of dealuminated samples shares in enhancing the amounts of ammonia adsorption. The amount of adsorbed ammonia molecules increases with the degree of exchange as can be seen in the curves from d to f. This was in agreement with the results obtained from the IR of ammonia adsorption. Apart from Bronsted sites that adsorb ammonia strongly (curve c), an enhancement was depicted upon modification for all samples. This was due to the ability of Cu^{2+} and Ni^{2+} to form amine complexes in solution as well as in zeolites [39]. Therefore, it is likely evaluating the amounts of diammine complexes by subtracting from those of cations free zeolites.

Following the models of Mortier and Sauer [40,41], it can be concluded that the acid strength rises with decreasing Al content of the framework (Al_f) in the dealuminated mordenites. The higher acid strength of the samples with a lower Al_f content should be reflected by a higher heat of

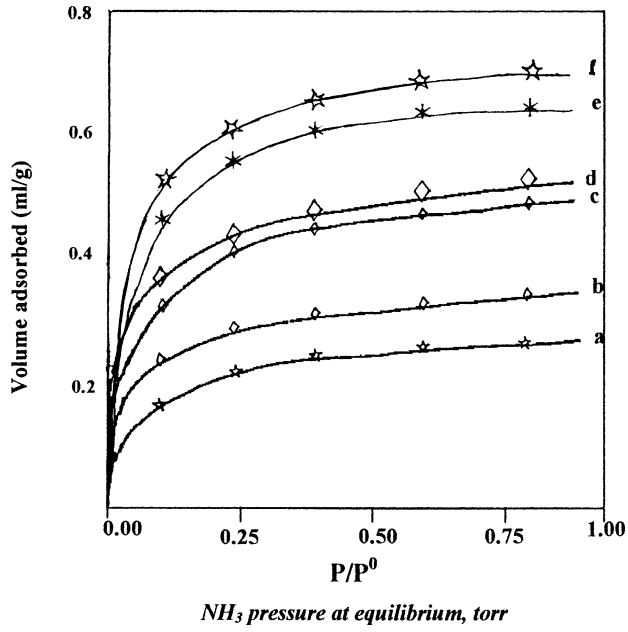

Fig. 6. Ammonia adsorption isotherms on nondealuminated and dealuminated mordenite zeolites: a, NaMSP; b, DML; c, DMH; d, 1 wt% Cu 1 wt% Ni/NaMSP; e, 1 wt% Cu 1 wt% Ni/DML; f, 1 wt% Cu 1 wt% Ni/DMH.

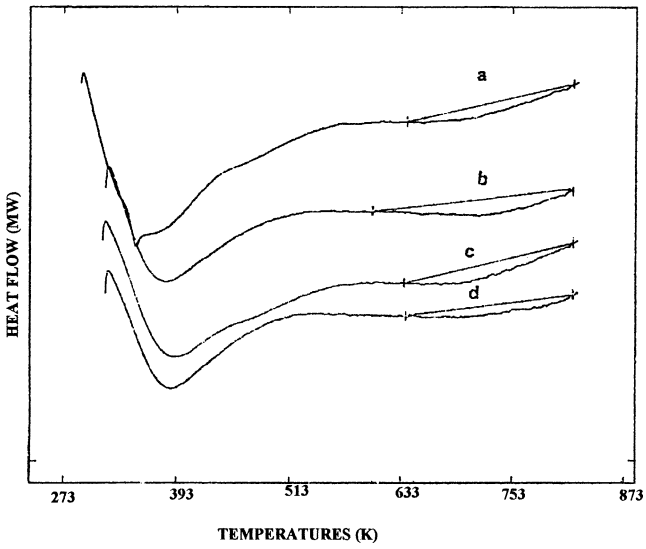

Fig. 7. DSC thermograms of NH_3 desorption from a, 1 wt% Cu 1 wt% Ni/NaMSP; b, 1 wt% Cu 1 wt% Ni/DML; c, 6 wt% Ni 1 wt% Cu/NaMSP; d, 6 wt% Ni 1 wt% Cu/DML.

Table 2
ΔH values obtained for DSC effects via ammonia desorption from some selected samples

Symbol	Sample	Peak 1			Peak 2	
		Range (K)	T_m (K)	ΔH ($J\,g^{-1}$)	T_m (K)	ΔH ($J\,g^{-1}$)
a	1Cu1Ni/NaMSP	323–553	351	230	711	13.6
b	1Cu1Ni/DML	323–510	381	116	739	22.6
c	6Ni1Cu/NaMSP	323–518	392	118	736	13.84
d	6Ni1Cu/DML	323–518	388	120	731	11.9

ammonia chemisorption and by a large number of the acid sites with a high chemisorption heat. As follows from Fig. 7, one can find qualitatively such a behavior. This was attained by measuring ΔH values for ammonia desorption, which are proportional to the number of acid sites. This figure depicts the thermograms of ammonia presorbing nondealuminated (curves a and c) and dealuminated-modified (curves b and d) samples. The thermograms of ammonia-presorbing NaMSP and DML samples containing 1Cu1Ni (curves a and b) are not identical in the sense that different temperatures are required to desorb ammonia from the samples (Table 2). This is due to the difference in binding forces between the acid sites of the samples and ammonia, i.e., acidity strength. The DSC effects due to desorption of ammonia from the weakest acid sites (hydrogen-bonding) appear between 343 and 563 K with a maximum at 351 K for thermogram a and at 381 K for thermogram b. This indicates the strength of the sites in the latter than on the former, although exceeding the magnitude of the ΔH value of thermogram a comparatively. In conformity with TPD results [42], it can be stated that the high temperature peak of a maximum in the 711–739 K range represents the desorption of ammonia from Bronsted acid sites. Consequently, Bronsted acid sites in thermogram b (dealuminated, $T_{max} = 739$ K) are markedly stronger than those in thermogram a (nondealuminated, $T_{max} = 711$ K). Moreover, the ΔH value for DSC effects obtained for Bronsted sites was higher in the former than in the latter (Table 2). On the other hand, significant differences were revealed between 6Ni1Cu/NaMSP and 6Ni1Cu/DML samples (curves c and d) either in the low or the high temperature ranges. Inspection of these samples indicates some ambiguous results, Table 2, especially for ΔH that indicates higher values for nondealuminated than for dealuminated, although their DSC maximum values are comparable. Indeed, the ΔH value in the low temperature range was higher in the former than in the latter due to an increase of the acid site number in the nondealuminated sample where no significant change was depicted in the high temperature range. This could be due to the nonaccessibility of the sites by NH_3 molecules because of the low basicity of ammonia molecules that cannot reach the deeply situated Bronsted acidic sites [43].

4. Conclusions

It was established for the first time using an IR tool (FTIR-PAS) that mordenite can be dealuminated as a result of encapsulation of Cu–Ni cations without performing any distinguished dealumination methods in advance. Hence, a band at 935(922) cm^{-1} was attained and assigned to Si–O–Si bonds. It has been shown that Cu has a dramatic effect on enhancing the dealumination process if compared with Ni. It was demonstrated that Ni replaces the protons in Si–(OH)–Al groups (3610 cm^{-1}), indicating an increase in Bronsted acidity by freeing the hydrogen protons. It was recognized that Cu is present in different channels other than the Bronsted silanol (3610 cm^{-1}) and most probably deep inside small channels. The adsorption capacity of ammonia was enlarged following dealumination and cation incorporation irrespective of the cation type.

Acknowledgment

The author thanks professor E.F. Vansant, University of Antwerp, Belgium, for his assistance in measuring this work samples by FTIR-photoacoustic techniques.

References

[1] C.T. Kresge, M.E. Leonowicz, W.J. Roth, J.C. Vartuli, J.S. Beck, Nature 359 (1992) 710.
[2] A. Sayari, I. Moudrakovski, Ch. Danumah, Ch.I. Ratcliffe, J.A. Ripmeester, K.F. Preston, J. Phys. Chem. 99 (1995) 16373.
[3] C.-Y. Chen, S.L. Burkett, H.-X. Li, M.E. Davis, Microporous Mater. 4 (1995) 1.
[4] K.M. Reddy, Ch. Song, Catal. Lett. 36 (1996) 103.
[5] A. Tuel, S. Gontier, Chem. Mater. 8 (1996) 114.
[6] S. Inagaki, Y. Yamada, Y. Fukushima, Stud. Surf. Sci. Catal. 105 (1997) 109.

[7] S.-C. Shen, S. Kawi, J. Phys. Chem. B 103 (1999) 8870.
[8] M.M. Mohamed, T.M. Salama, R. Ohnishi, M. Ichikawa, Langmuir 17 (2001) 5678;
A. Auroux, C. Guimon, F. Fitoussi, D. McQueen, B.H. Chiche, F. Fajula, P. Schulz, J. Catal. 161 (1996) 587.
[9] D. Freude, E. Brunner, H. Pfeifer, D. Prager, H.H. Jerschkewitz, U. Lohse, G. Oehlmann, Chem. Phys. Lett. 139 (1987) 325.
[10] K.-W. Lee, Y.-W. Lee, B.-H. Ha, J. Catal. 178 (1998) 328.
[11] M.D. Remy, G. Poncelet, J. Phys. Chem. 99 (1995) 773.
[12] D.A. Cadenhead, N.J. Wagner, R.L. Throp, in: Proc. 4th Int. Cong. Catal. (1968) I, (1971) 341.
[13] P.F. Carr, J.K.A. Clarke, J. Chem. Soc. A (1971) 985.
[14] V. Ponec, W.M.H. Sachtler, in: Proc. 5th Int. Cong. Catal. (1972) 2, (1973) 645.
[15] M.M. Mohamed, E.F. Vansant, J. Mater. Sci. 30 (1995) 4834.
[16] M.M. Mohamed, E.F. Vansant, Thermochim. Acta 230 (1993) 167.
[17] B. Ha, J. Guidot, D. Barthomeuf, J. Chem. Soc. Faraday Trans. 1 75 (1979) 1245.
[18] W.P.J.H. Jacobs, J.H.M.C. Van Wolput, R.A. Van Santen, J. Chem. Soc. Faraday Trans. 89 (1993) 1271.
[19] M. Maache, A. Janin, J.C. Lavalley, E. Benazzi, Zeolites 15 (1995) 507.
[20] F. Goovaerts, E.F. Vansant, P. De Hulsters, J. Gelan, J. Chem. Soc. Faraday Trans. 1 85 (1989) 3687.
[21] D.C. Sayle, C.R.A. Catlow, J.D. Gale, M.A. Perrin, P. Nortier, J. Phys. Chem. A 101 (1997) 3331.
[22] M.J. Van Niekerk, J.C.Q. Fletcher, C.T. Oconner, J. Catal. 138 (1992) 150.
[23] H.H. Baik, J. Guidot, D. Barthomeuf, J. Am. Chem. Soc. Faraday Trans. 1 75 (1979) 1245.
[24] M.M. Mohamed, G.M.S. El Shafei, J. Colloid Interface Sci. 175 (1995) 518.
[25] P. Tarte, Spectrochim. Acta 23A (1967) 2127.
[26] C. Lamberti, S. Bordiga, M. Salvalaggio, G. Spoto, A. Zecchina, F. Geolbaldo, G. Vlaic, M. Bellatreccia, J. Phys. Chem. B 101 (1997) 344.
[27] M.M. Mohamed, T.M. Salama, J. Colloid Interface Sci. 249 (2002) 104.
[28] H. Kosslick, V.A. Tuan, B. Parlitz, R. Fricke, Ch. Peuker, W. Storek, J. Chem. Soc. Faraday Trans. 89 (1993) 1131.
[29] J.-P. Shen, J. Ma, J. Guo, D.-Z. Jiang, E.-Z. Min, J. Chem. Soc. Faraday Trans. 91 (1995) 1835.
[30] D. Mc Queen, B.H. Chiche, F. Fajula, A. Auroux, C. Guimon, F. Fitoussi, P. Schulz, J. Catal. 161 (1996) 587.
[31] H. Kosslick, H. Landmesser, R. Fricke, J. Chem. Soc. Faraday Trans. 93 (1997) 1849.
[32] M.B. Sayed, R.A. Kydd, R.P. Cooney, J. Catal. 88 (1984) 137.
[33] A. Martin, U. Wolf, H. Brendt, B. Lucke, Zeolites 13 (1993) 309.
[34] H. Miessner, H. Kosslick, U. Lohse, B. Parlitz, V.-A. Yuan, J. Phys. Chem. 97 (1993) 9741.
[35] A.A. Davydov, Infrared Spectroscopy of Adsorbed Species on the Surface of Transition Metal Oxides, Wiley, 1990, pp. 28–36.
[36] J. Eng, C.H. Bartholomew, J. Catal. 171 (1997) 27.
[37] D.J. Parrillo, J.P. Fortney, R.J. Gorte, J. Catal. 153 (1995) 190.
[38] N.V. Filimonov, N.Yu. Lopatin, D.A. Sukhov, Kinet. Katal. 10 (1969) 458.
[39] A. Gedeon, J.L. Bonardet, J. Fraissard, J. Chem. Soc. Faraday Trans. 86 (1990) 413.
[40] W.J. Mortier, J. Catal. 55 (1978) 138.
[41] J. Sauer, in: Modeling of Structure and Reactivity in Zeolites, Academic Press, San Diego, 1993.
[42] W. Reschetilowski, B. Unger, K.-P. Wendlandt, J. Chem. Soc. Faraday Trans. 1 85 (1989) 2941.
[43] M.M. Mohamed, B.A. Abu-Zeid, Thermochim. Acta 359 (2000) 109.